

## Margatoxin increases dopamine release in rat striatum via voltage-gated $K^+$ channels

Alois Saria<sup>a,\*</sup>, Christine V. Seidl<sup>a</sup>, H.S. Fischer<sup>a</sup>, Robert O.A. Koch<sup>b</sup>, Stefan Telser<sup>a</sup>,  
Siegmond G. Wanner<sup>b</sup>, Christian Humpel<sup>a</sup>, Maria L. Garcia<sup>c</sup>, Hans-Günther Knaus<sup>b</sup>

<sup>a</sup> Department of Psychiatry, Neurochemical Unit, University Hospital, Anichstraße 35, 6020 Innsbruck, Austria

<sup>b</sup> Institute for Biochemical Pharmacology, Peter-Mayr Straße 1, 6020 Innsbruck, Austria

<sup>c</sup> Department of Membrane Biochemistry and Biophysics, Merck Research Laboratories, P.O. Box 2000, Rahway, NJ 07065, USA

Received 3 November 1997; accepted 25 November 1997

### Abstract

The distribution of iodinated margatoxin ( $[^{125}\text{I}]\text{margatoxin}$ ) binding sites in rat was investigated by autoradiography. Rat striatum expresses a high density of margatoxin binding sites and, therefore, the effects of margatoxin, charybdotoxin and iberiotoxin have been studied on  $[^3\text{H}]\text{dopamine}$  release from rat striatal slices in vitro. Margatoxin (0.1–100 nM) and charybdotoxin (10–1000 nM), but not iberiotoxin increased the spontaneous and the electrically evoked  $[^3\text{H}]\text{dopamine}$  release.  $[^3\text{H}]\text{dopamine}$  release by margatoxin was inhibited by tetrodotoxin and  $\omega$ -conotoxin GVIA, but not by atropine, naloxone,  $N^\omega$ -nitro-L-arginine and neurokinin or neurotensin receptor antagonists. In the buffer solution used for release experiments,  $[^{125}\text{I}]\text{margatoxin}$  labels a maximum of 0.12 pmol of sites/mg protein in rat striatal membranes with a  $K_d$  of 5 pM.  $[^{125}\text{I}]\text{margatoxin}$  binding was inhibited by margatoxin ( $K_i$  of 4 pM), charybdotoxin ( $K_i$  of 162 pM) but not by iberiotoxin. We conclude that inhibition of margatoxin-sensitive voltage-gated  $K^+$  channels increases  $[^3\text{H}]\text{dopamine}$  release demonstrating their role in repolarization of nigrostriatal projections. In contrast, iberiotoxin-sensitive, high-conductance  $\text{Ca}^{2+}$ -activated  $K^+$  channels are not involved in release of  $[^3\text{H}]\text{dopamine}$ . © 1998 Elsevier Science B.V.

**Keywords:**  $K^+$  channels; Dopamine release; Striatum, rat; Margatoxin; Iberiotoxin; (Binding)

### 1. Introduction

$K^+$  channels play crucial physiological roles in all neurons. Although a large number of different genes coding for these proteins have been cloned (Chandy and Gutman, 1995), it is still not widely established which particular gene product or combination controls the regulation of neurotransmitter release in individual neurons. One approach for studying  $K^+$  channel function in situ is to examine the effects of subtype-selective  $K^+$  channel blockers in defined neuron populations using functional assays.

An important class of  $K^+$  channel blockers comprises a number of scorpion-derived peptides (charybdotoxin, margatoxin, noxiustoxin, kaliotoxin and the agitoxins) which possess high affinity and selectivity for the *Shaker*-type

voltage-gated  $K^+$  channels  $K_v1.2$  and  $K_v1.3$  (Leonard et al., 1992; Werkman et al., 1992; Grissmer et al., 1994; Garcia et al., 1994). Two other  $K_v$  channels ( $K_v1.1$  and  $K_v1.6$ ) are also blocked by these toxins, but with significantly lower affinity, whereas  $K_v1.4$  and  $K_v1.5$  are completely insensitive (Stuhmer et al., 1989; Grissmer et al., 1994). In contrast, a homologous peptide derived from the venom of the scorpion *Buthus tamulus*, iberiotoxin, is selective for the high-conductance  $\text{Ca}^{2+}$ -activated  $K^+$  channel (Galvez et al., 1990; Knaus et al., 1996) without displaying any high affinity interaction with voltage-gated  $K^+$  channels. So far, only a few studies have employed these peptides to monitor modulation of neurotransmitter release, mostly at the neuromuscular junction (Vatanpour et al., 1993; Marshall et al., 1994; Vatanpour and Harvey, 1995).

Scorpion toxins have become an important tool for studying the pharmacological and biophysical properties of voltage-gated  $K^+$  channels and they exhibit a pharmaco-

\* Corresponding author. Tel.: +43-512-5043710; fax: +43-512-5043716; e-mail: alois.saria@uibk.ac.at

logical profile clearly distinct from the dendrotoxins (Grismer et al., 1994). However, functional experiments describing their effects on, for example, neurotransmitter release are widely lacking. In the present study, we investigated the distribution of [ $^{125}$ I]margatoxin binding sites in the rat forebrain by means of receptor autoradiography. As a result of the high expression levels of the binding site in the rat striatum, we have chosen this brain region for neurotransmitter release studies. In addition, we have established the pharmacological profile of the binding site under ionic strength conditions identical to those used in release experiments.

## 2. Materials and methods

### 2.1. Materials

Margatoxin, charybdotoxin and iberiotoxin were each expressed by recombinant methods in *E. coli* as part of fusion proteins and subsequently purified by cation exchange and C<sub>18</sub> reversed-phase chromatography by a method previously published (Garcia Calvo et al., 1993). Margatoxin was radiolabeled with [ $^{125}$ I]Na as previously described (Knaus et al., 1995). Glass fiber filters (GF/C) were from Whatman, Vienna, Austria. SR 140333, SR 48692 and SR 48968 were gifts from Sanofi, Montpellier, France. Polyethyleneimine and bovine serum albumin, tetrodotoxin, atropine, *N* $^{\omega}$ -nitro-arginine, *N*-[2-hydroxyethyl] piperazine-*N'*-[2-ethanesulfonic acid] and veratridine were from Sigma, Munich, Germany. Naloxone was from Aldrich, Vienna, Austria,  $\omega$ -conotoxin GVIA and dendrotoxin from RBI, Natwick, USA. Amersham hyperfilm and tritium-labeled dopamine were from Amersham, Buckinghamshire, UK. All other reagents were obtained from Merck, Darmstadt, Germany and were of analytical grade.

### 2.2. [ $^{125}$ I]margatoxin binding autoradiography

Male Sprague–Dawley rats (250–300 g) were sacrificed by cervical dislocation, their brains rapidly removed and placed for 90 s in isobutane, chilled to  $-40^{\circ}\text{C}$ . Thereafter, the brains were transferred for 30 min at  $-30^{\circ}\text{C}$  and stored in a sealed vial. 20  $\mu\text{m}$  sections were cut on a cryostat microtome (Leitz, Germany) and thaw-mounted onto gelatin-coated slides. Slides were stored at  $-30^{\circ}\text{C}$  for up to one month. For routine autoradiographies, sections were labeled in Krebs–Ringer buffer; 25.0 mM *N*-[2-hydroxyethyl]piperazine-*N'*-[2-ethanesulfonic acid], pH 7.4, 118 mM NaCl, 4.6 mM KCl, 1.17 mM MgSO<sub>4</sub>, 2.5 mM CaCl<sub>2</sub>, 1.17 mM NaH<sub>2</sub>PO<sub>4</sub>, 25.0 mM NaHCO<sub>3</sub>, containing 0.1% bovine serum albumin for 3 h at  $22^{\circ}\text{C}$  at a saturating [ $^{125}$ I]margatoxin concentration (20–23 pM). Nonspecific binding was determined in a series of adjacent sections by inclusion of 2 nM margatoxin. Sec-

tions were then rinsed twice for 30 min in ice-cold 20 mM Tris/HCl, pH 7.4, 150 mM NaCl, dipped twice in chilled distilled water and dried rapidly in a cold stream of air. Autoradiograms were obtained by exposing a sheet of film (Hyperfilm- $\beta$ max, Amersham) to labeled tissue sections in an X-ray cassette. After 4–6 h of incubation at room temperature, films were removed and developed using Kodak D-19 developer. To facilitate quantification, radiolabeled standards ([ $^{125}$ I]Microscales, Amersham) were included on each exposure. Under these experimental conditions, very low non-specific [ $^{125}$ I]margatoxin binding to the tissue sections was observed.

### 2.3. Release experiments

Male Sprague–Dawley rats (190–210 g) were decapitated and the striatum was dissected. Slices of a diameter of 400  $\mu\text{m}$  were cut by a vibratome and put into Krebs–Ringer buffer/bovine serum albumin/10 mM glucose buffer as described above. After preincubation of the pooled slices for 15 min in Krebs–Ringer buffer at  $37^{\circ}\text{C}$ , 2.5  $\mu\text{Ci}$  [ $^3\text{H}$ ]dopamine (specific activity 1.78 TBq/mmol) was added (final concentration 0.1  $\mu\text{M}$ ) and further incubated for 30 min, similar as described (Singer, 1988). The slices were placed into polyacrylamide chambers (1 slice per chamber, 3 chambers simultaneously) and superfused at  $37^{\circ}\text{C}$  with gassed (95% O<sub>2</sub>:5% CO<sub>2</sub>) Krebs–Ringer buffer as described previously (Saria et al., 1993). After an initial wash period of 45 min, 12–16 1-min fractions of 0.5 ml each were collected. Either margatoxin, charybdotoxin or iberiotoxin was added under normal perfusion conditions or during electrical field stimulation (100 V, 2 ms, rectangular pulses, 7 Hz generated by a Grass stimulator) for 30 s. In certain experiments, atropine (1  $\mu\text{M}$ ), *N* $^{\omega}$ -nitro-L-arginine (100  $\mu\text{M}$ ), naloxone (1  $\mu\text{M}$ ), SR 140333 (tachykinin NK<sub>1</sub> receptor antagonist, 5  $\mu\text{M}$ ), SR 48692 (tachykinin NK<sub>2/3</sub> receptor antagonist, 100 nM), SR 48968 (neurotensin receptor antagonist, 1  $\mu\text{M}$ ),  $\omega$ -conotoxin GVIA (1  $\mu\text{M}$ ) or tetrodotoxin (500 nM) were introduced to the superfusion medium. Before individual experiment termination, the slices were subjected to a K<sup>+</sup> pulse (60 mM) to ensure the viability of the preparation. Additionally, in some experiments, the control response was elicited by 5  $\mu\text{M}$  veratridine. In a separate set of experiments, 100 nM dendrotoxin (Research Biochemicals International, USA) or 100 nM dendrotoxin plus 100 nM margatoxin were superfused. In these experiments, 2-min fractions were collected and the collection time was 20–30 min. At the end of each experiment, the slices were collected and sonicated in Krebs–Ringer buffer. Radioactivity in slices and superfusates was determined by liquid scintillation counting. Reversed-phase high-performance liquid chromatography of some perfusates revealed that the major amount of radioactivity eluted in the position of unlabeled dopamine or dihydroxyphenyl acetic acid, not shown.

## 2.4. [ $^{125}$ I]margatoxin binding assay

The radioligand binding assay has been published previously (Knaus et al., 1995). The following modifications have been introduced: The assay buffer (1–2 ml) consisted of Krebs–Ringer buffer as described for the autoradiographic studies. *N*-[2-hydroxyethyl]piperazine-*N'*-[2-ethanesulfonic acid] was replaced by Tris/HCl, pH 7.4. Non-specific binding was defined in the presence of 2 nM recombinant margatoxin and incubation was carried out at 22–24°C, typically for 120 min. Receptor saturation studies were incubated for > 12 h. All serial toxin dilutions were performed in assay buffer. Employing these conditions around a  $K_d$  concentration of radioligand and receptor, nonspecific binding represented less than 1% of radioactivity added and specific binding was > 98% of total binding.

## 2.5. Protein determination and analysis of data

Protein was determined according to Bradford (1976). The results from saturation binding experiments were subjected to a Scatchard analysis and linear regression was

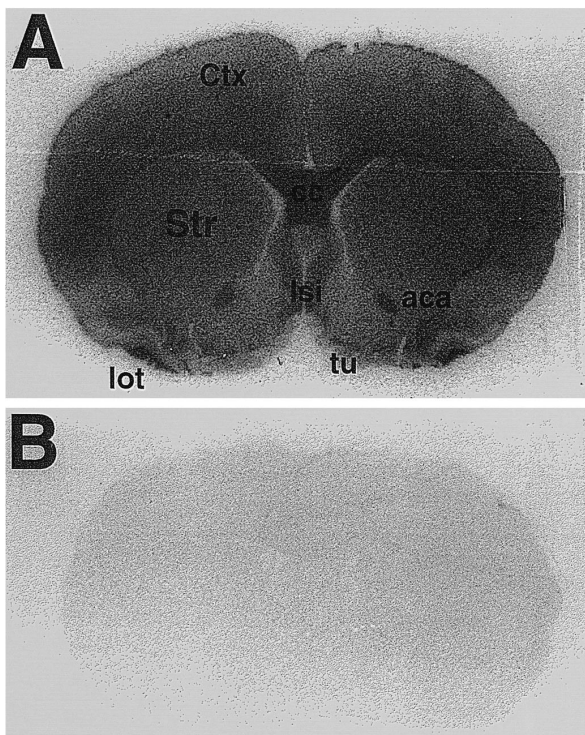


Fig. 1. Distribution of [ $^{125}$ I]margatoxin binding sites in rat forebrain. Sections of the rat forebrain were incubated with 21 pM [ $^{125}$ I]margatoxin in the absence (A) or presence (B) of 2 nM recombinant margatoxin and exposed on film for 4 h as described in Section 2. Binding of ligand appears as dark autoradiographic grains on a light background. Str, striatum; Ctx, cerebral neocortex; aca, anterior commissure; lot, lateral olfactory tract; cc, corpus callosum; tu, olfactory tubercle; lsi, lateral septal nucleus, intermediate.

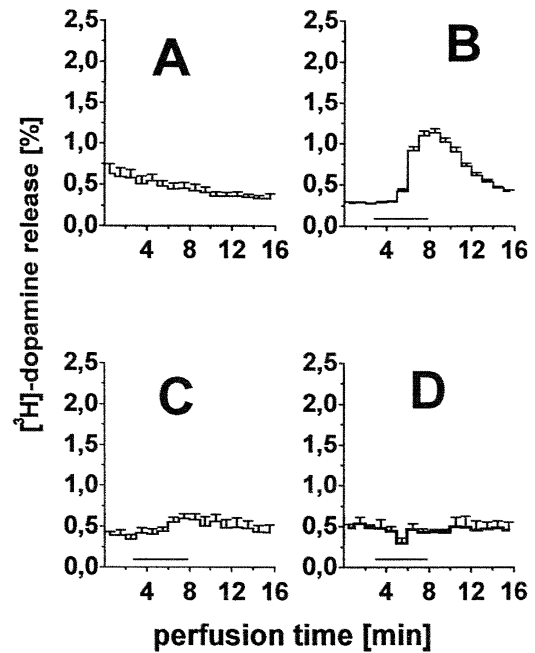


Fig. 2. Outflow of [ $^3$ H]dopamine from superfused striatal slices in vitro in the presence of  $K^+$  channel inhibitors. Each bar represents the [ $^3$ H]dopamine content of one fraction, expressed as % of the total radioactivity taken up by the respective slice during the preincubation period. Values are the means  $\pm$  S.E.M. The number of experiments is given in Table 2. The horizontal line below the graph indicates the superfusion period where the toxin was present in the medium. (A) Control (superfusion with buffer only); (B) 10 nM margatoxin; (C) 100 nM charybdotoxin and (D) 1  $\mu$ M iberiotoxin.

performed to obtain the equilibrium dissociation constant ( $K_d$ ) and maximal receptor concentration ( $B_{max}$ ). The correlation coefficient for these plots was typically > 0.98.

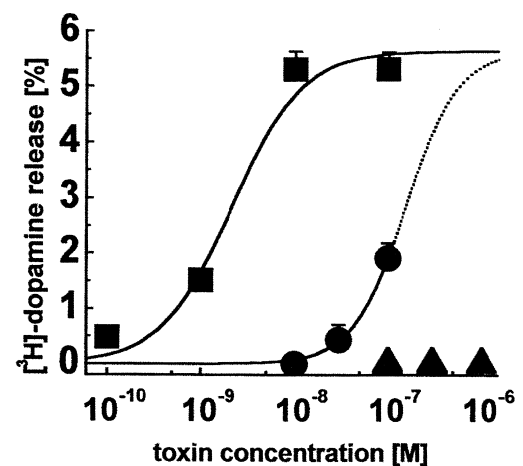


Fig. 3. Dose–response curves of total [ $^3$ H]dopamine release by margatoxin, charybdotoxin and iberiotoxin. Values represent means  $\pm$  S.E.M,  $n = 6$  for each concentration. Total release (%) was calculated as [ $^3$ H]dopamine released from fraction 4 to the end of the experiment, minus basal outflow (i.e. amount of [ $^3$ H]dopamine in the prestimulation fraction) and is expressed as percent of total [ $^3$ H]dopamine tissue content (i.e. radioactivity in the slice at the end of the experiment plus radioactivity in all collected fractions). Margatoxin (squares),  $EC_{50}$  2.1 nM; charybdotoxin (circles),  $EC_{50}$  152 nM; iberiotoxin (triangles), no effect.

Table 1

 $[^3\text{H}]$ dopamine outflow increased by electrical field stimulation in the presence of margatoxin and iberiotoxin

Stimulus/drug	Total release (% $[^3\text{H}]$ dopamine of tissue content)	<i>n</i>
Electrical field stimulation	1.16 ± 0.11	6
10 nM margatoxin	5.32 ± 0.32	36
10 nM margatoxin + electrical field stimulation	7.96 ± 0.67 <sup>a</sup>	10
300 nM iberiotoxin	0	3
300 nM iberiotoxin + electrical field stimulation	1.31 ± 0.27	5

Means ± S.E.M, *n* as indicated. Statistically significant differences were calculated with variance analysis and a post hoc (Scheffe-) test.<sup>a</sup>  $P \leq 0.001$  versus 10 nM margatoxin.

Data from competition experiments were computer-fitted to the general concentration–response equation (De Lean et al., 1978) and then analyzed by the method published previously (Linden, 1982) to determine  $K_i$  values. For statistical calculations of the release experiments, the Student's *t*-test or one-way analysis of variance and post hoc comparison with the Scheffe-test were applied where appropriate.

### 3. Results

#### 3.1. Distribution of $[^{125}\text{I}]$ margatoxin binding sites in rat forebrain sections

Under physiological buffer conditions (identical to the dopamine release experiments, see Section 3.2),  $[^{125}\text{I}]$ margatoxin binding to rat brain tissue sections occurred with high affinity and specificity (Fig. 1A and B). To achieve very low levels of non-specific binding, several long washing steps were performed, a procedure which was only feasible due to the fact that this radioligand exhibits a slow dissociation rate ( $k_{-1} \sim 10^{-4} \text{ s}^{-1}$  at 22°C; (Knaus et al., 1995). Specific  $[^{125}\text{I}]$ margatoxin binding to these sections was widely distributed and most brain regions were found to express margatoxin binding sites. The highest expression levels were detected in major white

matter tracts, e.g. the corpus callosum, the commissura anterior and the lateral olfactory tract. In addition, the cerebral cortex and the striatum yielded significant autoradiographic staining. This distribution profile prompted us to investigate the effects of margatoxin, charybdotoxin and iberiotoxin on dopamine release from nerve terminals of nigro-striatal projections, during either basal or electrically increased release.

#### 3.2. $[^3\text{H}]$ dopamine release induced by margatoxin, charybdotoxin and iberiotoxin

Superfusion of striatal slices in the presence of various concentrations of margatoxin significantly increased the outflow of  $[^3\text{H}]$ dopamine when compared to basal release (Figs. 2 and 3). A saturating margatoxin concentration (10 nM) (Fig. 3) released 5–6% of the tissue content of  $[^3\text{H}]$ dopamine (Table 1), which is about 11% of the releasable neurotransmitter pool as defined by depolarization with 60 mM  $\text{K}^+$  (Table 2). This amount of  $\text{K}^+$  induced a release of  $[^3\text{H}]$ dopamine of approximately 50% of total tissue content (Table 2). The threshold concentration of margatoxin for detectable  $[^3\text{H}]$ dopamine release was found to be 100 pM, while half-maximal release stimulation was observed at  $\sim 2 \text{ nM}$  toxin (Fig. 3). The release caused by 5  $\mu\text{M}$  veratridine was found to be approximately 12% of

Table 2

Effects of various drugs on margatoxin-evoked  $[^3\text{H}]$ dopamine release

Drug	Total release (% $[^3\text{H}]$ of tissue content)	<i>n</i>
60 mM $\text{K}^+$	49.4 ± 0.94	70
5 $\mu\text{M}$ veratridine	12.8 ± 1.53	68
10 nM margatoxin	5.32 ± 0.32	36
10 nM margatoxin + atropine 1 $\mu\text{M}$	4.55 ± 0.48	12
10 nM margatoxin + $N_\omega$ -nitro-L-arginine 100 $\mu\text{M}$	6.20 ± 0.46	10
10 nM margatoxin + naloxone 1 $\mu\text{M}$	5.79 ± 0.78	14
10 nM margatoxin + SR 140333 5 $\mu\text{M}$	4.96 ± 0.43	10
10 nM margatoxin + SR 48692 100 nM	5.39 ± 0.42	10
10 nM margatoxin + SR 48968 1 $\mu\text{M}$	6.41 ± 0.47	10
10 nM margatoxin + tetrodotoxin 500 nM	1.85 ± 0.21 <sup>b</sup>	6
10 nM margatoxin + $\omega$ -conotoxin GVIA 1 $\mu\text{M}$	2.40 ± 0.65 <sup>b</sup>	4

Means ± S.E.M, *n* as indicated. Statistically significant differences were calculated with variance analysis and a posthoc (Scheffe-) test.<sup>b</sup>  $P \leq 0.002$  versus 10 nM margatoxin.

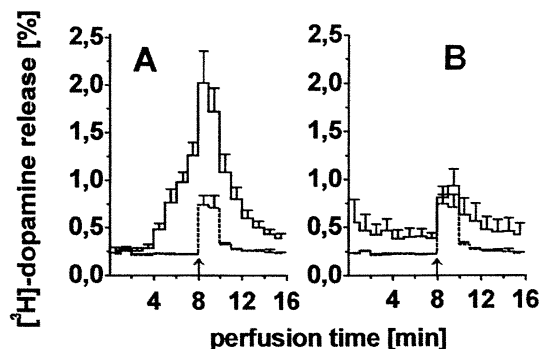


Fig. 4. Outflow of [ $^3\text{H}$ ]dopamine from superfused striatal slices induced by electrical field stimulation. The experiments were performed in the presence or absence (dashed line) of 10 nM margatoxin (A) or in the presence or absence of 300 nM iberiotoxin (B). Each bar represents the [ $^3\text{H}$ ]dopamine content of one fraction, expressed as % of the total radioactivity taken up by the respective slice during the preincubation period. Values are the means  $\pm$  S.E.M. The toxins were present in the medium between perfusion time 3 and 8, the arrow indicates the begin of the electrical field stimulation for 3 s. The number of experiments was 6 in absence of toxins (in A and B), 10 (margatoxin, A) and 5 (iberiotoxin, B).

the tissue content (Table 2). In order to investigate whether electrical stimulation of the slice preparation modulates the margatoxin effect, we monitored [ $^3\text{H}$ ]dopamine release in the absence or presence of toxin. Electrical field stimulation (3 s, 7 Hz) increased [ $^3\text{H}$ ]dopamine release about three times over basal outflow levels (Fig. 4A and B). When 10 nM margatoxin was applied during electrical field stimulation, the [ $^3\text{H}$ ]dopamine release was significantly higher than that with margatoxin or electrical field stimulation alone. After calculating the total amount of radioactivity released by electrical field stimulation in the presence of 10 nM margatoxin (area under the curve) and comparing this number to the sum of released radioactivity by either electrical field stimulation or 10 nM margatoxin alone, it became evident that the effect was higher than just additive (see Table 1,  $P < 0.05$ ).

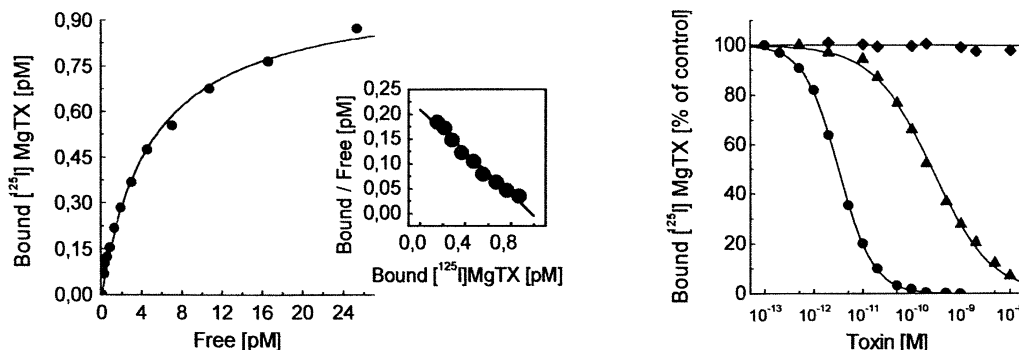


Fig. 5. Pharmacological profile of [ $^{125}\text{I}$ ]margatoxin binding to rat striatum synaptic plasma membrane vesicles. (A) Saturation binding analysis. Rat striatal synaptosomal membrane vesicles (6.0  $\mu\text{g}/\text{ml}$ ) were incubated with increasing concentration (0.28–26.2 pM) of [ $^{125}\text{I}$ ]margatoxin. The binding reaction was carried out at 22°C for 720 min in an assay volume of 2 ml. Specific binding (left, solid line) was assessed from the difference between total and nonspecific binding in the presence of 2 nM margatoxin. For this experiment, a  $K_d$  of 5.1 pM and a  $B_{\text{max}}$  value of 0.98 pM (corresponding to 0.12 pmol/mg of protein) was measured. Inset: binding data from (A) are presented in the form of a Scatchard representation. (B) Effects of margatoxin, charybdotoxin and iberiotoxin on [ $^{125}\text{I}$ ]margatoxin binding. Membrane vesicles (6  $\mu\text{g}/\text{ml}$ ) were incubated with 5 pM [ $^{125}\text{I}$ ]margatoxin in the absence or presence of increasing concentrations of either margatoxin (circles,  $\text{IC}_{50} = 3.2$  pM,  $n_H = 1.16$ ), charybdotoxin (triangles,  $\text{IC}_{50} = 219$  pM,  $n_H = 0.81$ ) or iberiotoxin (diamonds) at 22°C until equilibrium was achieved. Inhibition by margatoxin or charybdotoxin was assessed relative to an untreated control.

A dose-dependent increase of [ $^3\text{H}$ ]dopamine outflow was observed in the presence of charybdotoxin (Fig. 2C). The potency of charybdotoxin, however, was considerably lower than that of margatoxin and the amplitude of the effect displayed by margatoxin was not reached in the concentration range tested (Fig. 3). In contrast, iberiotoxin, a selective inhibitor of the high conductance  $\text{Ca}^{2+}$ -activated  $\text{K}^+$  channel, neither modulated basal [ $^3\text{H}$ ]dopamine outflow (Figs. 2 and 3), nor increased [ $^3\text{H}$ ]dopamine release induced by electrical field stimulation (Fig. 4B, Table 1).

### 3.3. Margatoxin-evoked [ $^3\text{H}$ ]dopamine release in the presence of various drugs

Additional controls were performed to demonstrate whether a direct action of margatoxin on the dopaminergic nerve terminal is responsible for the observed effects, since numerous neurotransmitters have been shown to modulate striatal dopamine release. We performed these experiments in order to rule out that the margatoxin-evoked [ $^3\text{H}$ ]dopamine is due to the release of a modulatory transmitter (acetylcholine, endogenous opioids, tachykinins, etc.) (Glowinski et al., 1988). Therefore, we monitored margatoxin-evoked [ $^3\text{H}$ ]dopamine release in the presence of antagonists of muscarinic acetylcholine receptors (1  $\mu\text{M}$  atropine), opiate receptors (1  $\mu\text{M}$  naloxone), tachykinin  $\text{NK}_1$ ,  $\text{NK}_2$  and  $\text{NK}_3$  receptors (5  $\mu\text{M}$  SR 140333 or 100 nM SR 48692), neurotensin receptors (1  $\mu\text{M}$  SR 48968), or nitric oxide synthase inhibitors (100  $\mu\text{M}$   $N^\omega$ -nitro-L-arginine) (Table 2). None of these compounds had a significant effect on the basal or the margatoxin-evoked [ $^3\text{H}$ ]dopamine release regardless of whether the toxin was investigated under basal release conditions, or during electrical field stimulation, indicating that a direct toxin effect is most likely to occur on the dopaminergic nerve terminal itself. Moreover, inhibition of voltage-gated sodium chan-

nels by tetrodotoxin strongly reduced the amount of [ $^3\text{H}$ ]dopamine released in the presence of margatoxin (Table 2).  $\text{Ca}^{2+}$ -free medium abolished the margatoxin-evoked [ $^3\text{H}$ ]dopamine release (data not shown), as did inhibition of N-type  $\text{Ca}^{2+}$  channels by  $\omega$ -conotoxin GVIA (Table 2). Taken together, these data provide additional support for a direct interaction of margatoxin (and also of charybdotoxin) on dopaminergic nerve terminals of nigro-striatal projections.

### 3.4. Characterization of [ $^{125}\text{I}$ ]margatoxin binding sites in rat striatal membranes

In order to establish the pharmacological profile of the striatal margatoxin binding site, we performed radioligand binding studies with the iodinated toxin. When crude rat striatal membrane vesicles were incubated in Krebs–Ringer buffer with increasing concentrations of [ $^{125}\text{I}$ ]margatoxin until equilibrium was achieved, the toxin associated with membranes in a concentration-dependent manner (Fig. 5A). Repetition of this experiment in the presence of 2 nM non-radiolabeled toxin resulted in a pattern of [ $^{125}\text{I}$ ]margatoxin association which is linearly dependent on radioligand concentration. The specific binding of margatoxin, defined as the difference between total radiolabeled toxin binding and binding in the presence of excess native peptide, was a saturable function of [ $^{125}\text{I}$ ]margatoxin concentration. A Scatchard analysis of these data (Fig. 5A, inset) indicated the presence of a single class of binding sites with a  $K_d$  of 5 pM and a  $B_{\text{max}}$  of 0.12 pmol/mg protein. At a concentration close to  $K_d$ , [ $^{125}\text{I}$ ]margatoxin binding to synaptic membrane protein was linear up to a concentration of 12  $\mu\text{g}$  protein/ml.

The pharmacological characteristics of the margatoxin binding site in striatum were further investigated. Thus, three structurally related toxins, margatoxin, charybdotoxin and iberiotoxin, were tested for their ability to modulate [ $^{125}\text{I}$ ]margatoxin binding. Both, margatoxin and charybdotoxin displayed complete inhibition of [ $^{125}\text{I}$ ]margatoxin binding to rat striatal membranes in a concentration-dependent manner. The means of the  $K_i$  values for these two toxins were 4.2 pM (margatoxin) and 162 pM (charybdotoxin). These numbers were found to be significantly lower than that determined in [ $^3\text{H}$ ]dopamine release experiments, a finding which might reflect incomplete toxin penetration into the striatal slice preparation. In marked contrast, iberiotoxin had no effect on margatoxin binding in brain at concentrations up to 10 nM (Fig. 5) and it did not cause any increase of [ $^3\text{H}$ ]dopamine release up to a final concentration of 1  $\mu\text{M}$  (see also Fig. 2).

### 3.5. [ $^3\text{H}$ ]dopamine release in the presence of dendrotoxin or dendrotoxin plus margatoxin

Dendrotoxin induced [ $^3\text{H}$ ]dopamine release of a similar magnitude as margatoxin (Fig. 6). When dendrotoxin was

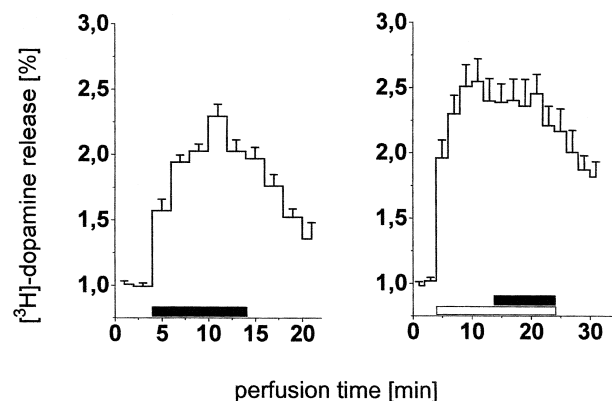


Fig. 6. Outflow of [ $^3\text{H}$ ]dopamine from superfused striatal slices in vitro in the presence of dendrotoxin (left) or dendrotoxin plus margatoxin (right). Each bar represents the [ $^3\text{H}$ ]dopamine content of one fraction, expressed as % of the total radioactivity taken up by the respective slice during the preincubation period. Values are the means  $\pm$  S.E.M. The number of experiments was 6 for each group. The black bar below the left graph indicates the superfusion period where 100 nM dendrotoxin was present in the medium. The open and the black bars below the right graph indicate the superfusion period where 100 nM dendrotoxin (open bar) and 100 nM margatoxin (filled bar), respectively, were present in the medium.

superfused on top of the margatoxin response, [ $^3\text{H}$ ]dopamine release was not further increased (Fig. 6).

## 4. Discussion

In the present study we report the distribution of [ $^{125}\text{I}$ ]margatoxin binding sites in the rat forebrain and investigate the effects of this toxin on dopamine release from nerve terminals of striatal afferents. Moreover, we establish the pharmacological profile of [ $^{125}\text{I}$ ]margatoxin binding to rat striatal membranes under physiological ionic strength conditions.

Previous binding studies have established [ $^{125}\text{I}$ ]margatoxin as a selective and very high affinity ligand for voltage-gated  $\text{K}^+$  channels in rat brain (Knaus et al., 1995). These experiments were performed under low salt conditions and, as a result, the toxin was shown to bind with very high affinity ( $K_d \sim 0.1$  pM). To be able to compare the binding properties of [ $^{125}\text{I}$ ]margatoxin with the effect of the toxin on [ $^3\text{H}$ ]dopamine release as presented herein, we performed all our experiments (including the autoradiographies) under physiological ionic concentrations. Employing these conditions, [ $^{125}\text{I}$ ]margatoxin binds to its binding site with a  $K_d$  of 5 pM. This very high affinity of [ $^{125}\text{I}$ ]margatoxin binding results from very slow toxin dissociation (Knaus et al., 1995), in clear contrast to [ $^{125}\text{I}$ ]charybdotoxin binding kinetics (Vazquez et al., 1990). This property of [ $^{125}\text{I}$ ]margatoxin constitutes an advantage for performing autoradiographic studies and, even more importantly, for immunoprecipitation studies. These autoradiographies reveal that [ $^{125}\text{I}$ ]margatoxin binding is widely distributed in rat forebrain. The highest expression

levels were detected in major fiber tracts, e.g. the corpus callosum, commissura anterior and the lateral olfactory tract. This distribution was very similar to the one reported for [ $^{125}$ I]charybdotoxin (Gehlert et al., 1992; Gehlert and Gackenhaimer, 1993) and, moreover, it correlated reasonably well with the immunocytochemical staining pattern of the voltage-gated  $K^+$  channel  $K_v1.2$  (Wang et al., 1994). Besides strong [ $^{125}$ I]margatoxin expression in major fiber tracts, the toxin binding site was also found in the cerebral neocortex and the striatum. Since  $K_v1.2$  represents a predominant *Shaker*-type  $K^+$  channel in rat brain (Scott et al., 1994) and both margatoxin and charybdotoxin have been characterized as high-affinity inhibitors of this channel, this finding provides speculative support that  $K_v1.2$  might serve as a main component of the toxin binding site in rat striatum. Currently, there is limited information available concerning the expression of  $K_v1.3$  protein in the rat forebrain except for the olfactory bulb (Veh et al., 1995). This voltage-gated  $K^+$  channel is also potentially blocked by margatoxin and charybdotoxin, a fact that prompted us to investigate the contribution of this  $K^+$  channel subunit to [ $^{125}$ I]margatoxin binding (see below). Since margatoxin and charybdotoxin are known to block voltage-dependent  $K^+$  channels, whereas iberiotoxin, that did not displace [ $^{125}$ I]margatoxin binding, is a selective inhibitor of high-conductance  $Ca^{2+}$ -activated  $K^+$  channels, these data strongly suggest that the margatoxin binding site is functionally associated with a voltage-dependent  $K^+$  channel which serves as an important repolarization pathway in dopaminergic nigro-striatal projections.

Based on these findings, we restricted all further experiments to a singular neuro-anatomically well defined region, the striatum. One of the striatal input systems is comprised of the dopaminergic nigro-striatal projection originating in the substantia nigra, pars compacta and terminating in the striatum. Superfusion of a [ $^3$ H]dopamine-preloaded striatal slice preparation with margatoxin resulted in reproducible neurotransmitter release, which had a rapid onset and reached a maximum at  $\sim 10$  nM toxin. Half-maximal stimulation of release was observed at 2 nM margatoxin. In these experiments, margatoxin was of lower potency when compared to radioligand binding studies performed under identical conditions. A possible explanation to account for this discrepancy could be due to the fact that this highly charged hydrophilic toxin displays poor penetration into the slice preparation, reaching high peptide levels only in the superficial cell layers of the slice. The margatoxin effect was observed under basal release conditions suggesting that inhibition of repolarization of spontaneously active dopaminergic axons and terminals by margatoxin is sufficient to cause a significant stimulation of [ $^3$ H]dopamine outflow.

When charybdotoxin-induced [ $^3$ H]dopamine release was compared to that of margatoxin, a considerably lower potency was determined ( $\sim 100$ -fold). This finding is in good agreement with radioligand binding data in which

charybdotoxin also displayed lower potency. The effect of charybdotoxin on [ $^3$ H]dopamine release is consistent with the fact that this toxin was shown to be effective in retarding action potential repolarization in striatal neurons (Flores Hernandez et al., 1994). In contrast, iberiotoxin did not cause any [ $^3$ H]dopamine release and in conjunction with this finding, did not displace [ $^{125}$ I]margatoxin binding to rat striatal synaptic plasma membrane vesicles. The inability of iberiotoxin to increase [ $^3$ H]dopamine release from nerve terminals of nigro-striatal projections indicates that high-conductance  $Ca^{2+}$ -activated  $K^+$  channels do not significantly contribute to repolarization in these dopaminergic neurons. This is in agreement with the observation that *slo* channel mRNA, which encodes the pore-forming subunit of the high-conductance  $Ca^{2+}$ -activated  $K^+$  channel, was not detected in in situ hybridization experiments in the substantia nigra pars compacta (Knaus et al., 1996). Taken together, these findings support the idea that margatoxin and charybdotoxin exert their effects on [ $^3$ H]dopamine release through inhibition of voltage-gated  $K^+$  channels and, moreover, that the margatoxin binding site provides an important repolarization pathway in dopaminergic nigro-striatal neurons.

The margatoxin-evoked [ $^3$ H]dopamine release was reduced by  $\omega$ -conotoxin GVIA and tetrodotoxin indicating that the mechanism of action involves rapid sodium entry and  $Ca^{2+}$ -dependent exocytosis. Other putative modulators of dopamine release (Glowinski et al., 1988) were ineffective, indicating that the margatoxin effect in our model results from a direct action on prejunctional dopaminergic terminals and not subsequently to release of acetylcholine, neurokinins, neurotensin, endogenous opiates or nitric oxide. As expected from the previous literature, dendrotoxin also increased dopamine release. The combination of saturating concentrations of margatoxin and dendrotoxin, however, did not further augment the response. This indicated that both toxins utilize the same channel subtype ( $K_v1.2$  and/or  $K_v1.1$ ) in our model. The exact subtype composition of margatoxin binding sites has not been established yet, but future studies using specific antibodies against various subunits should solve this problem.

We conclude that inhibition of margatoxin-sensitive voltage-gated  $K^+$  channels increases [ $^3$ H]dopamine release demonstrating their role in repolarization of nigrostriatal projections. The channels involved are largely the same as those inhibited by dendrotoxins (Pongs, 1992). In contrast, iberiotoxin-sensitive, high-conductance  $Ca^{2+}$ -activated  $K^+$  channels are not involved in release of [ $^3$ H]dopamine.

## Acknowledgements

This study was supported by the Austrian Science Foundation grant # F00206. The technical help of Mrs. Astrid Saria is gratefully acknowledged. H.G.K. was supported by grants from the Austrian Science Foundation (S6611-MED and P11187-MED) and an APART fellow-

ship from the Austrian Academy of Sciences. We gratefully thank Dr. Robert Slaughter and Dr. Gregory J. Kaczorowski, Department of Membrane Biochemistry and Biophysics, Merck Research Laboratories, Rahway, NJ, for providing [ $^{125}$ I]margatoxin and serving as valuable discussion partners.

## References

- Bradford, M.M., 1976. A rapid and sensitive method for the quantitation of microgram quantities of protein utilizing the principle of protein-dye binding. *Anal. Biochem.* 72, 248–254.
- Chandy, K.G., Gutman, G.A., 1995. Voltage-gated potassium channel genes. In: North, R.A. (Ed.), *Handbook of Receptors and Channels: Ligand and Voltage-Gated Ion Channels*. CRC Press, Boca Raton/Ann Arbor/London/Tokyo, pp. 1–71.
- De Lean, A., Munson, P.J., Rodbard, D., 1978. Simultaneous analysis of families of sigmoid curves: Application to bioassays, radioligand assay and physiological dose–response curves. *Am. J. Physiol.* 4, E97–E102.
- Flores Hernandez, J., Galarraga, E., Pineda, J.C., Bargas, J., 1994. Patterns of excitatory and inhibitory synaptic transmission in the rat neostriatum as revealed by 4-AP. *J. Neurophysiol.* 72, 2246–2256.
- Galvez, A., Gimenez Gallego, G., Reuben, J.P., Roy Contancin, L., Feigenbaum, P., Kaczorowski, G.J., Garcia, M.L., 1990. Purification and characterization of a unique, potent peptidyl probe for the high conductance calcium-activated potassium channel from venom of the scorpion *Buthus tamulus*. *J. Biol. Chem.* 265, 11083–11090.
- Garcia Calvo, M., Leonard, R.J., Novick, J., Stevens, S.P., Schmalhofer, W., Kaczorowski, G.J., Garcia, M.L., 1993. Purification, characterization and biosynthesis of margatoxin, a component of *Centruroides margaritatus* venom that selectively inhibits voltage-dependent  $K^+$  channels. *J. Biol. Chem.* 268, 18866–18874.
- Garcia, M.L., Garcia Calvo, M., Hidalgo, P., Lee, A., MacKinnon, R., 1994. Purification and characterization of three inhibitors of voltage-dependent  $K^+$  channels from *Leiurus quinquestriatus* var. *hebraeus* venom. *Biochemistry* 33, 6834–6839.
- Gehlert, D.R., Gackenheimer, S.L., 1993. Comparison of the distribution of binding sites for the potassium channel ligands [ $^{125}$ I] apamin, [ $^{125}$ I] charybdotoxin and [ $^{125}$ I] iodoglyburide in the rat brain. *Neuroscience* 52, 191–205.
- Gehlert, D.R., Gackenheimer, S.L., Robertson, D.W., 1992. Autoradiographic localization of [ $^{125}$ I] charybdotoxin binding sites in rat brain. *Neurosci. Lett.* 140, 25–29.
- Glowinski, J., Cheramy, A., Romo, R., Barbeito, L., 1988. Presynaptic regulation of dopaminergic transmission in the striatum. *Cell Mol. Neurobiol.* 8, 7–17.
- Grissmer, S., Nguyen, A.N., Aiyar, J., Hanson, D.C., Mather, R.J., Gutman, G.A., Karmilowicz, M.J., Auperin, D.D., Chandy, K.G., 1994. Pharmacological characterization of five cloned voltage-gated  $K^+$  channels, types  $K_v1.1$ ,  $1.2$ ,  $1.3$ ,  $1.5$  and  $3.1$ , stably expressed in mammalian cell lines. *Mol. Pharmacol.* 45, 1227–1234.
- Knaus, H.G., Koch, R.O.A., Eberhart, A., Kaczorowski, G.J., Garcia, M.L., Slaughter, R.S., 1995. [ $^{125}$ I] Margatoxin, an extraordinarily high affinity ligand for voltage-gated  $K^+$  channels in mammalian brain. *Biochemistry* 34, 13627–13634.
- Knaus, H.G., Schwarzer, C., Koch, R.O.A., Eberhart, A., Kaczorowski, G.J., Glossmann, H., Wunder, F., Pongs, O., Garcia, M.L., Sperk, G., 1996. Distribution of high-conductance Ca-activated  $K^+$  channels in rat brain: Targeting to axons and nerve terminals. *J. Neurosci.* 16, 955–963.
- Leonard, R.J., Garcia, M.L., Slaughter, R.S., Reuben, J.P., 1992. Selective blockers of voltage-gated  $K^+$  channels depolarize human T-lymphocytes: Mechanism of the antiproliferative effect of charybdotoxin. *Proc. Natl. Acad. Sci. USA* 89, 10094–10098.
- Linden, J., 1982. Calculating the dissociation constant of an unlabeled compound from the concentration required to displace radioactive binding by 50%. *J. Cyclic Nucleotide Res.* 8, 163–172.
- Marshall, D.L., Vatanpour, H., Harvey, A.L., Boyot, P., Pinkasfeld, S., Doljansky, Y., Bouet, F., Menez, A., 1994. Neuromuscular effects of some  $K^+$  channel blocking toxins from the venom of the scorpion *Leiurus quinquestriatus hebraeus*. *Toxicon* 32, 1433–1443.
- Pongs, O., 1992. Structural basis of voltage-gated  $K^+$  channel pharmacology. *Trends Pharmacol. Sci.* 13, 359–365.
- Saria, A., Troger, J., Kirchmair, R., Fischer-Colbrie, R., Hogue-Angeletti, R., Winkler, H., 1993. Secretoneurin releases dopamine from rat striatal slices: A biological effect of a peptide derived from secretogranin II (chromogranin C). *Neuroscience* 54, 1–4.
- Scott, V.E., Muniz, Z.M., Sewing, S., Lichtinghagen, R., Parcej, D.N., Pongs, O., Dolly, J.O., 1994. Antibodies specific for distinct  $K_v$  subunits unveil a heterooligomeric basis for subtypes of alpha-dendrotoxin-sensitive  $K^+$  channels in bovine brain. *Biochemistry* 33, 1617–1623.
- Singer, E.A., 1988. Transmitter release from brain slices elicited by single pulses: A powerful method to study presynaptic mechanisms. *Trends Pharmacol. Sci.* 9, 274–276.
- Stuhmer, W., Ruppersberg, J.P., Schroter, K.H., Sakmann, B., Stocker, M., Giese, K.P., Perschke, A., Baumann, A., Pongs, O., 1989. Molecular basis of functional diversity of voltage-gated potassium channels in mammalian brain. *EMBO J.* 8, 3235–3244.
- Vatanpour, H., Harvey, A.L., 1995. Modulation of acetylcholine release at mouse neuromuscular junctions by interaction of three homologous scorpion toxins with  $K^+$  channels. *Br. J. Pharmacol.* 114, 1502–1506.
- Vatanpour, H., Rowan, E.G., Harvey, A.L., 1993. Effects of scorpion (*Buthus tamulus*) venom on neuromuscular transmission in vitro. *Toxicon* 31, 1373–1384.
- Vazquez, J., Feigenbaum, P., King, V.F., Kaczorowski, G.J., Garcia, M.L., 1990. Characterization of high affinity binding sites for charybdotoxin in synaptic plasma membranes from rat brain. Evidence for a direct association with an inactivating, voltage-dependent, potassium channel. *J. Biol. Chem.* 265, 15564–15571.
- Veh, R.W., Lichtinghagen, R., Sewing, S., Wunder, F., Grumbach, I.M., Pongs, O., 1995. Immunohistochemical localization of five members of the  $K_v1$  channel subunits: Contrasting subcellular locations and neuron-specific co-localization in rat brain. *Eur. J. Neurosci.* 7, 2189–2205.
- Wang, H., Kunkel, D.D., Schwartzkroin, P.A., Tempel, B.L., 1994. Localization of  $K_v1.1$  and  $K_v1.2$ , two  $K$  channel proteins, to synaptic terminals, somata, and dendrites in the mouse brain. *J. Neurosci.* 14, 4588–4599.
- Werkman, T.R., Kawamura, T., Yokoyama, S., Higashida, H., Rogawski, M.A., 1992. Charybdotoxin, dendrotoxin and mast cell degranulating peptide block the voltage-activated  $K^+$  current of fibroblast cells stably transfected with NGK1 ( $K_v1.2$ )  $K^+$  channel complementary DNA. *Neuroscience* 50, 935–946.